ISSN 0022-0930, Journal of Evolutionary Biochemistry and Physiology, 2022, Vol. 58, Suppl. 1, pp. S107–S124. © Pleiades Publishing, Ltd., 2022.

EXPERIMENTAL PAPERS

Integrative Mathematical Model of Electrical, Metabolic and Mechanical Processes in Human Cardiomyocytes

N. A. Balakina-Vikulova[a],* and L. B. Katsnelson[a],**

[a] *Institute of Immunology and Physiology, Russian Academy of Sciences, Yekaterinburg, Russia*
**e-mail: n.vikulova@iip.uran.ru*
***e-mail: leonidkatsnelson51@gmail.com*

Received September 22, 2022

Revised November 11, 2022

Accepted November 15, 2022

Abstract—A complex sequence of electrical and mechanical processes at different levels of the heart organization provides its pumping function. The force generation by the contractile proteins of cardiomyocytes requires energy expenditure. In addition, some ion transport mechanisms in the cell consume ATP to redistribute ions between various cell structures and transfer them to the extracellular space during the excitation-contraction of the cardiomyocyte. Intracellular mitochondria are involved in ATP synthesis. We have developed an integrative mathematical model of a human left ventricular cardiomyocyte, which describes the processes of electromechanical coupling in the cell, the process of ATP synthesis in mitochondria in the tricarboxylic acid cycle, and the utilization of ATP by the activities of various pathways. The integrative model shows that a change in the mechanical conditions of cardiomyocyte contraction in the normal state (for example, a change in its initial length or applied load) not only affects the time course of the action potential in the cell but also modulates the processes associated with the ATP production and utilization. The mechano-dependence of mitochondrial energetics is provided by a complex system of mechano-electric, mechano-calcium and mechano-metabolic direct links and feedbacks. Our simulations reveal that despite the mechano-dependent changes, the ATP level remains within the range of values characteristic of healthy myocardium.

DOI: 10.1134/S0022093022070122

Keywords: myocardium, electromechanical coupling, biomechanics, metabolism, mechano-electric feedback, mathematical model

INTRODUCTION

The mechanisms of excitation-contraction coupling (ECC) and mechano-electrical feedback (MEF) are widely studied at different levels of heart organization, both in physiological and numerical experiments. Intracellular mechanisms of ECC provide cardiomyocyte contraction and force generation in response to an electrical stimulus. The sequence of the excitation-contraction processes in the heart cell is well studied. It includes a change in the amplitude of membrane currents, the redistribution of calcium ions in the cell, the formation of calcium complexes with calcium-binding proteins, and the attachment/detachment of force-generating cross-bridges between actin and myosin filaments.

MEF mechanisms provide the effect of

mechanical conditions of myocardial contraction on electrical processes in the heart muscle. For example, a change in preload and afterload in the cardiac cycle leads to a change in the duration of the action potential (AP) in cardiomyocytes [1]. It is well known that even in a healthy heart the myocardial tissue is very heterogeneous. The heterogeneity of the myocardium is manifested in the different structural and functional properties of the cardiomyocytes. The mechanisms of ECC and MEF ensure effective excitation of heterogeneous myocardial tissue, coordinated contraction of cardiomyocytes and generation of mechanical stress [2, 3].

The function of cardiac tissue significantly depends on the energy of ATP consumed during the force generation by the cardiomyocyte and in the pump- and carrier-mediated ion transport processes. The study of metabolic processes in the myocardium is necessary for the complex investigation of normal and pathologically damaged myocardium. It is especially important in cases where pathological changes are directly related to the insufficient blood supply to the heart tissue (hypoxia or ischemia) resulting in a decrease in the ATP level in the cardiomyocyte.

Electro-mechano-metabolic relationships in cardiomyocytes are very complex. Their integrative contribution to myocardium work is hard to assess even in the most comprehensive experimental study. Attempts are being made to clarify these relationships for local interactions. For example, Cortassa et al. simultaneously studied the effect of the frequency of contraction on the rate of oxygen absorption and the force developed by the trabecula of rats [4].

Brandes and Bers investigated the effect of muscle work increase after sarcomere lengthening and stimulation frequency rise on a fall in mitochondrial NADH concentration [5]. Numerous studies have been conducted on the effect of the activation of ATP-dependent potassium current on cellular function and its role in pathological conditions of the myocardium (see review [6]).

With the help of mathematical models tested on the available experimental data, we can follow the direct and inverse relationships between the observed phenomena, predict the effects of changes in external conditions on the behaviour of a cardiomyocyte, and put forward hypotheses for further experimental verification.

The aim of our work was to develop an integrative mathematical model that allows the study of the electro-mechano-metabolic relationships in human ventricular cardiomyocytes in a healthy and pathologically altered myocardium. To develop a new model, we used modules that are well-verified models describing electromechanical coupling and metabolic processes in cardiomyocytes (see next section for more details). At the first stage of our research, we studied the activity of cardiomyocytes under normal conditions. To clarify the electro-mechano-metabolic relationships in this model, we altered the mechanical conditions of cardiomyocyte contraction. In particular, we examined how the initial length of the cardiomyocyte altered the time course of intracellular processes during stationary contractions under periodic stimulation (steady-state contractions) and how the applied load under which cardiomyocyte shortening occurs alters cardiomyocyte activity in a contraction cycle. The integrative model makes it possible to draw conclusions about the mechanisms of changes observed when mechanical conditions change.

INTEGRATIVE MATHEMATICAL MODEL

The developed integrative mathematical model of the cardiomyocyte of the human left ventricle consists of modules describing calcium handling, electrical, metabolic and mechanical processes. The modules are interconnected by the description of the mechanisms that provide direct and feedback links between them. The electromechanical module is represented by the recently developed human cardiomyocyte model *TP+M* [7], which, in turn, combines the electrophysiological model of human cardiomyocyte *ten Tusscher-Panfilov-2006* [8] and the previously developed module of mechanical activity of the heart muscle and calcium kinetics in cardiomyocytes [9]. The description of metabolic processes in mitochondria and intracellular ATPases is taken from the integrative model *Cortassa-2006* [4], the species specificity of which has not been determined. The integration of the human cardiomyocyte *TP+M* model and the metabolic module

was performed by replacing the description of electrical and mechanical intracellular processes inherited in the *Cortassa-2006* model from the *Rice* model [10, 11] with the equations of the electromechanical *TP+M* model. For a full list of model equations, a rheological scheme of the mechanical module of the model, as well as a list of parameters and initial values of phase variables see the Supplementary Material.

The *electrophysiological* module describes potassium, calcium and sodium ion membrane currents and membrane potential (V) in the cardiomyocyte. The rate of change of the membrane potential is defined as follows:

$$\frac{dV}{dt} = -\frac{1}{C_m}\left(\sum_{k=6} i^k_{K^+} + \sum_{n=2} i^n_{Na^+} + \sum_{m=3} i^m_{Ca^{2+}} + i_{NaK} + i_{NaCa} + i_{\text{stim}}\right), \quad (1)$$

where the first term is the sum of all potassium ion currents through the cell membrane (including the ATP-dependent potassium current $i_{K,ATP}$ added when combining the models; the latter is necessary for further use of the suggested mathematical model to study effects of cardiac ischemia); the second term is the sum of all sodium ion currents through the cell membrane; the third term is the sum of all calcium ion currents through the cell membrane (including the current of the ATP-consuming membrane calcium pump i_{pCa}); i_{NaK} is the current of the ATP-consuming sodium-potassium membrane pump; i_{NaCa} is the current of the sodium-calcium exchange mechanism on the cell membrane; i_{stim} is the stimulating current simulating the arrival of excitation from a neighboring cell.

The kinetics of calcium in cardiomyocytes is directly related to both the AP generation (equation (1)) and the force generation. The change in intracellular calcium concentration (Ca_i) is described by the differential equation:

$$\frac{dCa_i}{dt} = Ca_{i_{bufc}} \cdot \left(\frac{V_{SR}}{V_C}(I^{SR}_{up} - I^{SR}_{leak}) - I_{xfer} - \frac{i_{bCa} + i_{pCa} - 2\cdot i_{NaCa}}{V_C \cdot F} - \frac{dCaTnC}{dt} - \frac{V_{mito}}{V_C}\cdot(V^{mit}_{NaCa} - V^{mit}_{uni})\right), \quad (2)$$

where the multiplier $Ca_{i_{bufc}}$ occurs with a quasi-stationary description of the total calcium concentration associated with intracellular buffer ligands other than troponin C in the *TP+M* model (for more details, see [12]). The total concentration of intracellular buffer ligands was reduced if compared with the *TP+M* model since calcium exchange with mitochondria is extracted in a separate module in the new integrative model; I^{SR}_{up}, I^{SR}_{leak} are the flow of ATP-dependent calcium uptake by the pump on the membrane of the sarcoplasmic reticulum (*SR*) and the flow of passive leakage from *SR* into the cytosol; I_{xfer} is the diffusion of calcium from the dyadic space, into which calcium enters through L-type calcium channels during cell excitation (see the Supplementary Material); i_{bCa} is the background calcium current through the cell membrane; $\frac{dCaTnC}{dt}$ is the rate of the binding of *calcium* to *troponin C*; V^{mit}_{NaCa} is the calcium flow through the sodium-calcium exchanger on the mitochondrial membrane (the term was added during integration with the metabolic model); V^{mit}_{uni} is the calcium flow through the calcium uniporter on the mitochondrial membrane (the term added during integration with the metabolic model); V_C, V_{SR} are *cytoplasm* and *SR* volumes; $\frac{V_{mito}}{V_C}$ is the ratio of the volumes of mitochondria and cytoplasm (from the *Cortassa-2006* model); F is the Faraday constant.

In the integrative model, a link between electrophysiological and metabolic blocks emerges based on ATP dependence and competitive ADP inhibition of i_{pCa}, i_{NaK} and I^{SR}_{up} currents. To implement these dependencies, the description of the activity of each mechanism includes additional modulating multipliers represented in the same form as in the original *Cortassa-2006* model [4].

The mechanical activity of a cardiomyocyte is described by a rheological scheme that contains a contractile element (CE) that simulates the activity of cardiomyocyte sarcomeres and elements that represent the viscoelastic properties of the

heart muscle [12] (Fig. 1 in Supplementary Material). The contractile element is responsible for the generation of the active force of cardiomyocytes and sarcomere shortening due to the formation of cross-bridges during the attachment of myosin heads to actin filaments. The formation of cross-bridges during the contractile cycle of the sarcomere is regulated by calcium, which forms complexes with troponin C (*CaTnC*) located along the thin filament. A key feature of the developed integrative model, inherited from the *TP+M* model is the consideration of cooperative mechanisms that make the kinetics of CaTnC dependent on the number of attached force-generating cross-bridges (N_{XB}) [9]. In particular, the decay of the CaTnC complex becomes slower with an increase in the number of cross-bridges and/or with an increase in the number of other CaTnC complexes formed near this complex.

The force generated by the contractile element (F_{CE}) of the rheological scheme of the model is proportional to the number of attached cross-bridges N_{XB}:

$$F_{CE} = \lambda \times \rho_{\upsilon} \times N_{XB}, \quad (3)$$

where λ is proportionality coefficient, ρ_{υ} is the force generated by one cross-bridge, depending on the sliding velocity of thin filaments along thick filaments.

In isometric contractions, the length of the cardiomyocyte (L_{sample}) remains constant:

$$L_{\text{sample}} = \text{const}. \quad (4)$$

At the same time, the lengths of all elements of the rheological scheme, including the contractile element, elastic and viscous elements, change due to differences in their biomechanical properties.

The total force developed by the cardiomyocyte (F_{sample}) is determined by the forces that develop the elements of the rheological scheme during its shortening and lengthening. In isometric mode (Fig. 2 in Supplementary Material), this force can be written based on the structure of the rheological scheme, as equal to the force of an external in-series elastic element (F_{XSE}) whose length (l_3) is changed due to the deformation of other elements:

$$F_{\text{sample}} = F_{XSE} = \beta_3 \cdot (e^{\alpha_3 \cdot l_3} - 1), \quad (5)$$

where α_3 and β_3 are coefficients characterizing the elastic force of the external in-series element XSE.

Isotonic afterloaded contractions of a cardiomyocyte (Fig. 2 in Supplementary Material) are characterized by the constancy of the generated force, which is equal to some fixed value ρ:

$$F_{\text{sample}} = \rho. \quad (6)$$

L_{sample} varies under isotonic conditions depending on the applied load.

A link between mechanical and metabolic block is implemented in the integrative model similar to the *Cortassa-2006* model. An ATP dependence of the sarcomere force generation process is not considered in the new integrative model. Experimental data indicate a low sensitivity of force generation to changes in ATP in a wide range [13]. Nevertheless, the model takes into account the ATP consumption by actomyosin ATPase in the overall change in the ATP cytosolic concentration (ATP_i) (see equation (8) below). In the *Cortassa-2006* model, the rate of ATP hydrolysis by actomyosin ATPase is proportional to the normalized rate of formation of cross-bridges at several stages of their attachment to functional units A7+Tn+Tm (7 monomers of actin + troponin + tropomyosin). The description of the process of formation of cross-bridges in the *Cortassa-2006* model is adopted from the *Rice* model [14]. Our mechanical module of the *TP+M* model describes the kinetics of cross-bridges cycling by a simpler scheme than in the *Rice* model. Therefore, we postulated that the rate of ATP hydrolysis by actomyosin ATPase (V_{AM}) is proportional to the number of detachments of the cross-bridges, which, in turn, is proportional to the number of cross-bridges at any given moment:

$$V_{AM} = N_{XB} \cdot V_{AM}^{\max} \cdot \left(1 + \frac{K_{m,\,ATP}^{ATP}}{ATP_i} \cdot \left(1 + \frac{ATP_i}{K_{i,\,AM}}\right)\right)^{-1}, \quad (7)$$

where $K_{m,\,ATP}^{ATP}$ is the half-saturation constant; $K_{i,AM}$ is the inhibition constant of actomyosin ATPase by cytosolic ADP (ADP_i).

The coefficient of the maximum rate of ATP hydrolysis by actomyosin ATPase ($V_{AM}^{\max}$) was selected so that the amplitude of the rate change in

the cycle corresponded to that in the *Cortassa-2006* model.

The *metabolic* module of the integrative model inherited from the *Cortassa-2006* model contains a description of the mechanisms involved in supporting the energy needs of the cardiomyocyte. Specifically, this module describes the complete cycle of mitochondrial ATP production, ATP/ADP transport across the mitochondrial membrane, and calcium exchange between cytosol and mitochondria.

The differential equation describing the change in the ATP cytosolic concentration directly consumed in the ECC processes is as follows:

$$\frac{dATP_i}{dt} = V_{ANT}\cdot\frac{V_{mito}}{V_C} - V_{CK}^{mito} - (V_{AM} + 0.5\cdot I_{up}^{SR} + (i_{NaK} + i_{pCa})\cdot\frac{C_m}{V_C\cdot F}), \quad (8)$$

where V_{ANT} is ADP/ATP exchange between cytosol and mitochondria via a carrier on the mitochondrial membrane; V_{CK}^{mito} is the rate of synthesis of creatine phosphate from ATP by mitochondrial creatine kinase.

The model assumes that the total concentration of ATP and ADP nucleotides in the cytosol is a constant value, which is 8 mM under normal conditions. Then the concentration of cytosolic ADP is defined as follows:

$$\mathrm{ADP}_i = 8.0 - \mathrm{ATP}_i. \quad (9)$$

Mitochondrial concentration of ADP (ADP_m),

$$\frac{dATP_m}{dt} = V_{ANT} - V_{ATPase} - V_{SL}, \quad (10)$$

changes due to the flow of ADP into the mitochondria through V_{ANT} the binding of ADP on the active centers of ATP synthase (V_{ATPase}) and the ATP consumption during one of the reactions of the Krebs cycle when succinyl-CoA converts to succinate (V_{SL}).

The total concentration of ATP and ADP nucleotides in the mitochondria in the model is also constant and is 1.5 mM under normal conditions. The concentration of mitochondrial ATP (ATP_m) is defined as follows:

$$\mathrm{ATP}_m = 1.5 - \mathrm{ADP}_m. \quad (11)$$

Mitochondria are able to uptake and release free intracellular calcium via calcium uniporters and sodium-calcium antiporters. This process can be considered calcium buffering. Calcium buffering by mitochondria is not the main storage in the cardiomyocyte, but it plays an important role in the relationship between electrical, mechanical, and metabolic processes in the integrative model, both because it affects the kinetics of free intracellular calcium and because calcium ions indirectly control important mitochondrial functions. The change in the concentration of mitochondrial calcium (Ca_m) is written as:

$$\frac{dCa_m}{dt} = f_m\cdot(V_{NaCa}^{mit} - V_{uni}^{mit}), \quad (12)$$

where f_m is the fraction of free Ca_m; V_{NaCa}^{mit} and V_{uni}^{mit} are the calcium flows across the mitochondrial membrane (see equation (2)).

The translocation of calcium, nucleotides and protons through the mitochondrial membrane is electrogenic. Hence, the mitochondrial membrane potential changes ($\Delta\Psi_m$):

$$\frac{d\Delta\Psi_m}{dt} = -\frac{1}{C_{mito}}\cdot(-V_{HNe} - V_{HFe} + V_{Hu} + V_{Hleak} + V_{ANT} + V_{NaCa}^{mit} + 2\cdot V_{uni}^{mit}), \quad (13)$$

where C_{mito} is the inner membrane capacitance; the first four terms relate to proton transfer by various mechanisms located on the mitochondrial membrane (respiratory chain carriers, ATP synthase, etc.); the remaining flows are defined in the descriptions to the equations (8) and (10).

Mitochondrial calcium not only affects the mitochondrial membrane potential but also stimulates the production of NADH in the Krebs cycle, increasing the production of ATP.

Combining models required changing some of the input parameters to reproduce the experimental data used in the *TP+M* model verification and to obtain realistic steady states of the output characteristics of the new model. For example, the initial simulation of the contraction-relaxation cycles in the new integrative model showed that the amplitude of the change in the concentration of free cytosolic calcium in the cycle (calcium transient) dropped. The level of free cytosolic calcium obtained was lower than in experiments on normal human myocardium [15] and then in the

TP+M model [12]. The available amount of free calcium in the cytosol could not provide mechanical activation of cardiomyocytes. The amplitude and time course of the force generated in the developed model were outside the experimental ranges [15–17]. To obtain the amplitude of the calcium transient sufficient for the development of force in steady-state contractions the rate of calcium translocation through the calcium uniporter on the mitochondrial membrane V_{uni}^{mit} was reduced compared to the value used in the *Cortassa-2006* model (from 0.0275 to 0.007 mM/ms) (see Fig. 3 in Supplementary Material). This change made it possible to ensure an adequate level of diastolic and systolic calcium and the number of cross-bridges, which was sufficient to generate isometric force and contractions in isotonic conditions.

In addition, the maximum calcium uptake rate by the SR pump V_{maxup} (see Table 3 in Supplementary Material) was reduced compared with the TP+M model (from 0.00765 to 0.001 mM/ms). Because of this reduction, the contribution of calcium uptake by the SR pump I_{up}^{SR} to the change in the rate of intracellular ATP decreased (equation (8)). This change was necessary since, during the initial integration of the *TP+M* model and the *Cortassa-2006* metabolic model, the ATP cytosolic level in steady state contractions fell to values unrealistic for non-pathological conditions [18]. Our model analysis showed that the greatest contribution to the ATP consumption is in the SR pump. Therefore, a change in the SR uptake rate allowed us to preserve the physiological values of ATP in the cytosol.

These changes, as well as additional species-specific fine-tuning of the parameters of the mechanical and electrical modules, allowed us to obtain a model that correctly reproduces the amplitude-time characteristics of isometric contractions and corresponding AP recorded in experiments on human heart muscles [15–17, 19].

Thus, we have constructed an integrative model of electro-mechano-metabolic activity of a human cardiomyocyte. The model consists of 44 differential equations and additional algebraic formulas. To describe the processes in the model, 225 constants are used, the physiological relevance of which has been evaluated and largely validated based on experimental data during the development of each of the three main modules combined in this model. The Runge–Kutta method was used with a step of 0.0025 ms for numerical integration of the model.

To obtain steady state isometric contractions, 400 cycles were calculated with applying the stimulating current i_{stim} (equation (1)) with a frequency of 1 Hz.

In a series of experiments to study the length dependence of the virtual cardiomyocyte activity, we compare the time course of various output characteristics obtained for each given initial length of L_{sample} in the last (steady-state) cycle.

When studying the load dependence of the virtual cardiomyocyte activity, the output characteristics of isotonic contractions obtained under different loads ρ (equation (6)) on the first cycle after the last steady-state isometric cycle were compared.

The software for calculating the model and visualizing the results is written in the Borland Delphi 7.0 environment.

RESULTS

Length dependence of cardiomyocyte function in isometric twitches

Using the integrative mathematical model of the human ventricular cardiomyocyte, we studied the effect of the initial length (i.e. preload) on electrical, mechanical and metabolic processes in the cardiomyocyte in steady-state contractions at a stimulation frequency of 1 Hz. Similar experiments were carried out on the human myocardium using isolated trabeculae from donors' hearts, but only the mechanical response of the preparation was registered [20]. Previously, we simulated isometric contractions of a cardiomyocyte using the electromechanical *TP+M* model [12]. We repeated those mechanical conditions for numerical experiments in the new integrative model. In each experiment of the series, under the same initial conditions, a different initial length L_{sample} of the virtual preparation was set. The length L_{sample} varied from 80% to 95% of $L_{\max}$ (where $L_{\max}$ corresponds to the length of the sar-

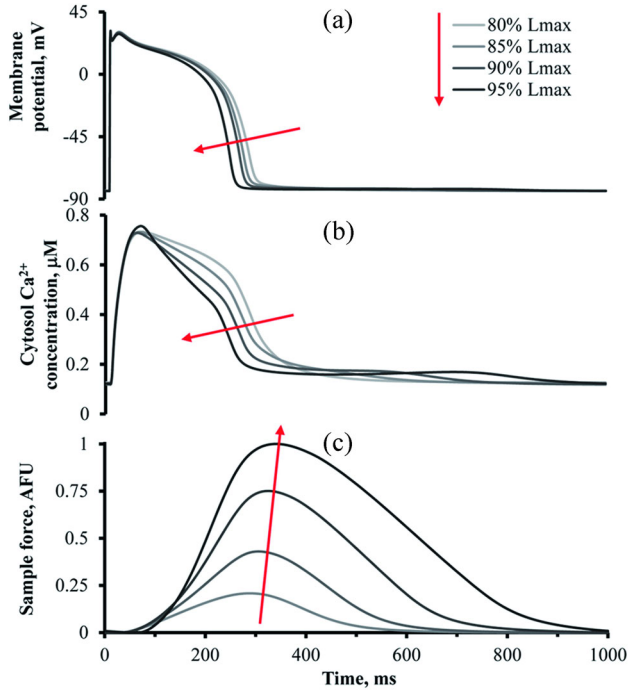

Fig. 1. Length dependence in the integrative model. The time course of the membrane potential (a), changes in the cytosolic concentration of free calcium (b) and the active isometric force of the virtual cell (c) in steady state contractions at different initial lengths of 80–95% of L_{max}. AFU (arbitrary force unit) is used after force normalization to the maximum value of isometric force observed at initial length L_{sample} = 95% L_{max}. The arrows show the direction of displacement of the curves with increasing length.

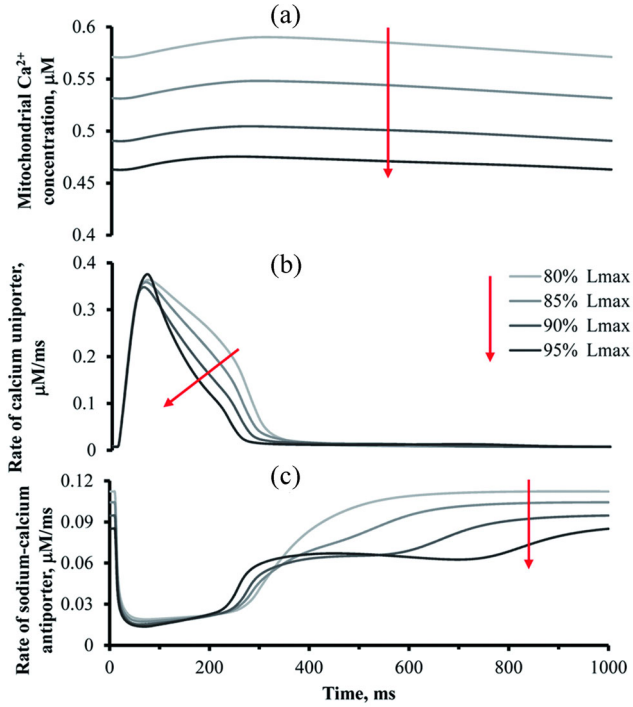

Fig. 2. Length dependence in the integrative model. The time course of changes in mitochondrial calcium concentration (a), the rates of the calcium uniporter V_{uni}^{mit} (b) and the sodium-calcium antiporter V_{NaCa}^{mit} (c) across the mitochondrial membrane in steady-state contractions of the virtual cardiomyocyte at different initial lengths of 80–95% of L_{max}. The arrows show the direction of displacement of the curves with increasing length.

comere 2.2 μm). The results obtained in steady-state contractions of the virtual preparations are compared.

Figure 1 shows the time course of AP changes, free cytosolic calcium concentration and active isometric force at different preloads in the new integrative model. The model reproduces the main characteristic dependences on the initial length. Specifically, it has been shown that the maximum value of the developed isometric force and the time to reach this value increases with increasing length (Fig. 1c). The duration of the relaxation phase of the developed force also increases with increasing length. The observed changes are consistent with experimental observations [20]. The AP duration is smaller at a bigger L_{sample} (Fig. 1a). These changes, as we have already shown earlier, are related to the MEF mechanisms. Since the model takes into account the cooperative mechanisms of the dependence of the formation and dissociation of calcium-troponin complexes on the mechanical conditions of contraction, the free cytosolic calcium concentration changes its temporal and amplitude characteristics in response to a change in the initial length (equation (2), Fig. 1b). These changes, in turn, affect the calcium-dependent ion currents that determine AP development (equation (1)). This part of the results is repeated and consistent with the results obtained using the *TP+M* model [12].

With an increase in preload, a decrease in the level of free mitochondrial calcium is observed (Fig. 2a). In particular, when the length changes from 80 to 95% of L_{max}, the diastolic mitochondrial calcium concentration decreases from 0.57 to 0.46, that is, by about 20%. These changes are directly related to alterations in the time course of free cytosolic calcium (Fig. 1b) since the integrative model takes into account the mechanisms of

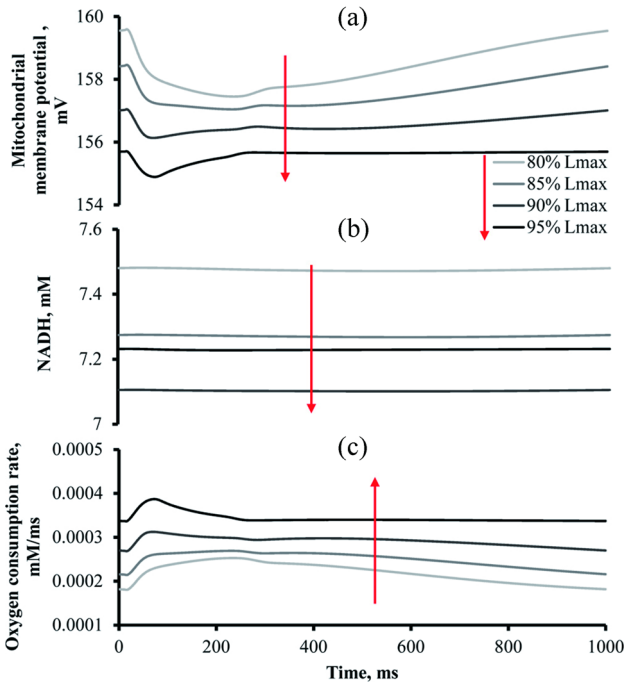

Fig. 3. Length dependence in the integrative model. The time course of changes in the potential on the mitochondrial membrane (a), NADH concentration (b) and oxygen consumption rate (c) in the mitochondria in steady-state contractions of a virtual cardiomyocyte at different initial lengths of 80–95% of L_{max}. The arrows show the direction of displacement of the curves with increasing length.

calcium ion exchange between the cytosol and mitochondria (equations (2) and (12)). Figure 2b shows that the decrease in the mitochondrial calcium concentration over a bigger length is caused by a shorter period of calcium uptake into the mitochondria through a mitochondrial calcium uniporter (V_{uni}^{mit}, equations (2) and (12)), which passes calcium into the mitochondria along an electrochemical gradient. This mechanism is active until the free cytosol calcium concentration remains above the diastolic level. The calcium transient shortening is accompanied by a shortening of the uniporter activity period.

Simultaneously with the calcium uniporter, an antiporter works on the mitochondrial membrane (V_{NaCa}^{mit}, equations (2) and (12)). It removes calcium from the mitochondria in exchange for sodium ions under normal conditions. Its rate depends on both the concentration of free cytosolic calcium (Ca_i) and the concentration of mitochondrial calcium (Ca_m). Figure 2c shows that the diastolic rate of the antiporter V_{NaCa}^{mit} in the steady state differs at different initial lengths of the virtual preparation. The bigger the initial length, the less the rate is.

In parallel with the increased flow through the mitochondrial calcium uniporter, the sodium-calcium mitochondrial antiporter is inhibited by increased cytosolic calcium. This change reveals a rapid decrease in antiporter rate compared to diastolic values (Fig. 2c). Then, the antiporter rate gradually increases, enhancing the calcium removal from the mitochondria. Moreover, in steady state contractions, the bigger the initial length L_{sample}, the slower the return of the antiporter rate to diastolic values.

The calcium uniporter and the sodium-calcium antiporter are potential-dependent and, in turn, themselves affect the mitochondrial membrane potential. According to equation (13), length-dependent changes in calcium flows through these mechanisms should affect the time course of the mitochondrial potential in steady-state isometric contractions. Figure 3a shows that the potential on the mitochondrial membrane varies in diastole depending on the initial length. With an increase in length from 80% to 95% of L_{max}, mitochondrial membrane potential during the diastole decreases by 4 mV (2.5%). This decrease value is greater than the magnitude of mitochondrial membrane potential change during the cycle. The profile of changes in mitochondrial potential during the contractile cycle also differs depending on the initial length: the smaller the initial length, the longer it takes for the mitochondrial potential to return from systolic to diastolic values.

Since the proton motive force (not shown) in the metabolic model is directly proportional and linearly dependent on the mitochondrial membrane potential, the same qualitative changes in the time course of the proton motive force are observed as in the mitochondrial membrane potential when the initial length changes in the isometric steady-state cycles.

The concentration of NADH, which is involved in the oxidation of respiratory substrates to carbon dioxide and water, is slightly decreased at bigger initial lengths in the steady-state isomet-

ric contractions (Fig. 3b). This correlates with a decrease in the mitochondrial calcium concentration (Fig. 2a). In particular, as the length increases from 80% to 95% of L_{max}, the diastolic NADH concentration decreases by about 3%. It should be noted that the absolute changes in NADH levels during steady-state contractions at a given length compared to other lengths are much more pronounced than the changes in NADH concentration during a cycle at a given length.

Such changes in the mitochondrial membrane potential, proton motive force and NADH concentration lead to quantitative and qualitative changes in the rate of oxygen absorption (Fig. 3c) and the rate of hydrogen transport through the mitochondrial membrane (not shown). The longer the initial length of the virtual preparation, the higher these rates, and the shorter the period of decline to diastolic values.

The ATP formation in the mitochondria is determined by the amount of ADP available for synthesis (equation (10)). This ADP enters the mitochondria from the cytosol in exchange for synthesized ATP (process rate V_{ANT}) and is consumed during the operation of F1F0-ATP synthase (process rate V_{ATPase}) and in the reaction in the citric acid cycle (during the catalysis of the conversion of succinyl-CoA to succinyl) (process rate V_{SL}).

All three processes (V_{ANT}, V_{ATPase} and V_{SL}) have different rates in steady-state isometric contractions at different initial lengths. The balance of these three mechanisms ensures an increase in the mitochondrial ADP concentration with a bigger initial length. Since ADP+ATP is a constant value in the model (equation (11)), then with a bigger initial length, the steady-state concentration of ATP synthesized by mitochondria is lower (Fig. 4b). Note that if the differences in the mitochondrial ATP diastolic level between the lengths of 80 and 90% of L_{max} are only about 6%, then a further change in the initial length by another 5% (with a change in length from 90 to 95% of L_{max}) leads to a more significant drop in the mitochondrial ATP diastolic level by 19%.

The synthesized ATP enters the cytosol from the mitochondria (Fig. 4a). In steady-state contractions, its level almost does not decrease with

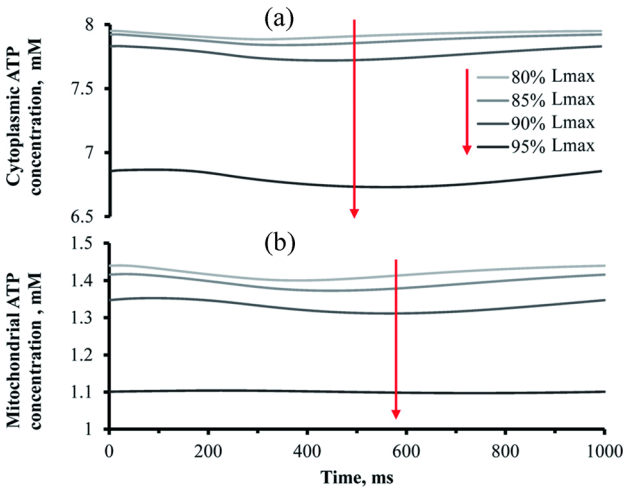

Fig. 4. Length dependence in the integrative model. The time course of changes in the concentration of ATP in the cytosol (a) and in the mitochondria (b) in steady-state contractions of the virtual cardiomyocyte at different initial lengths of 80–95% of L_{max}. The arrows show the direction of displacement of the curves with increasing length.

increasing length from 80 to 90% of L_{max}. The concentration difference for diastolic ATP values in the cytosol for these lengths is 2%. In steady-state contractions at a length of 95% of L_{max}, the ATP cytosolic concentration decreases more significantly, and its decrease is 14% compared to values at a length of 80% of L_{max}.

The energy from ATP decomposition into ADP and inorganic phosphates is used in the cell by the SR calcium pump, sodium-potassium pump, sarcolemmal calcium pump and actomyosin interaction in the process of generating mechanical force. As already mentioned, in the equations describing the operation of ion transport mechanisms (i_{pCa}, i_{NaK} current and V_{up}^{SR} flow), their ATP dependence and ADP competitive inhibition are determined by special multipliers. As the initial length increases, these multipliers decrease with changes in ATP and ADP levels. The multiplier associated with the calcium SR uptake is the most sensitive to changes in the level of ATP in the cytosol. When changing the initial length from 80 to 90% of L_{max}, its contribution to changing V_{up}^{SR} is reduced by 2.4%, and with a further increase in length to 95% of L_{max} is reduced by another 16%. The multipliers determining the

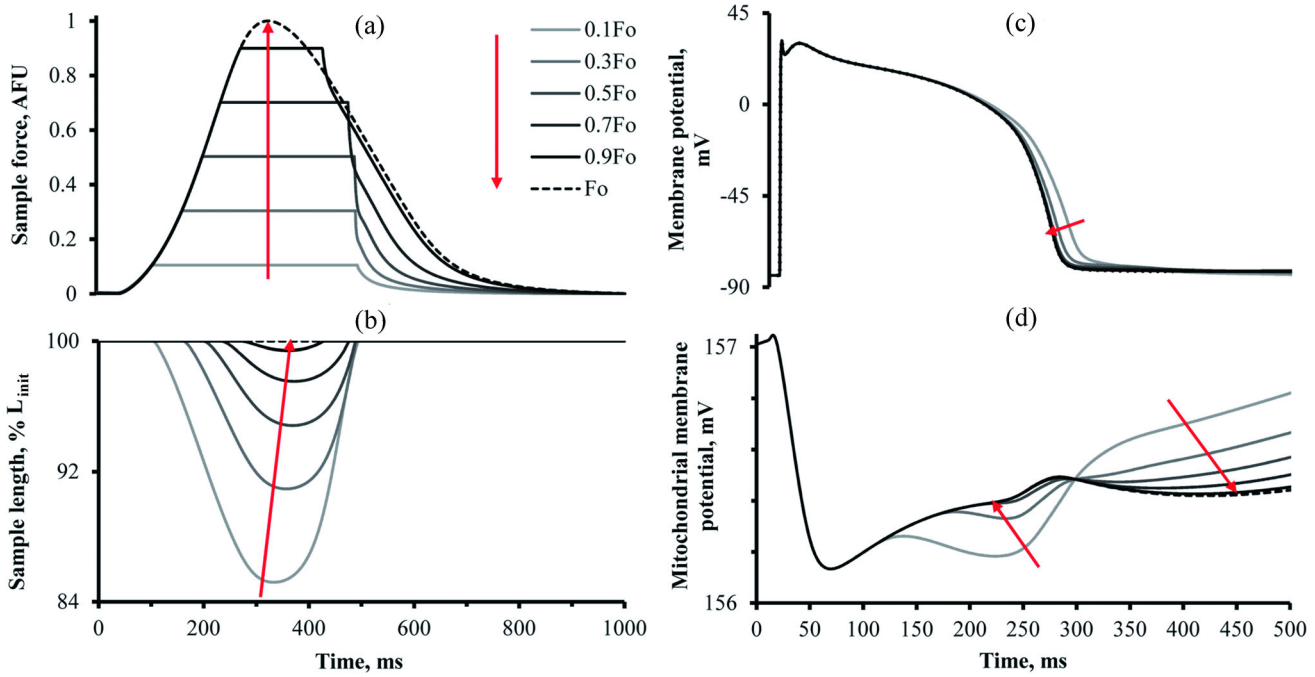

Fig. 5. Load dependence in the integrative model. The time course of changes in the force (a) and length (d) of the virtual cardiomyocyte, and the cell membrane potential (c) and the mitochondrial membrane potential (d) in steady-state isometric contraction (dotted lines) and at different afterloads (solid lines). The initial length of the virtual cardiomyocyte L_{init} = 90% L_{max}. AFU (arbitrary force unit) is used after force normalization to F_0, which represents the maximum value of isometric force developed by the cardiomyocyte at the initial length L_{init}. The afterload level is set in fractions of F_0. The arrows show the direction of displacement of the curves with increasing afterload. Note, panels (c) and (d) show the first 500 ms of the cycle.

ATP dependence of the currents i_{pCa} and i_{NaK} change slightly within 0.5–1.3% with an increase in the initial length.

Load dependence of cardiomyocyte activity in afterload twitches

The integrative model was used to study electromechanical and metabolic phenomena in cardiomyocytes during their contraction under afterload conditions. We considered the isotonic contraction of a virtual cardiomyocyte under afterload (see equation (6)) in the next cycle after the steady-state isometric twitch (Fig. 5, dotted lines). The initial length of the cardiomyocyte was $L_{sample}(t = 0) = L_{init} = 90\%\ L_{max}$ in the experiment shown. In the series of experiments presented in Fig. 5, the afterload varied from values of $\rho = 0.9F_0$ for heavily loaded shortening (dark grey lines) to $\rho = 0.1F_0$ for lightly loaded shortening (light grey lines), where F_0 is the maximum value of the isometric force (dotted lines) developed by the cardiomyocyte at the initial length L_{init}. The proposed numerical experiment makes it possible to evaluate the instantaneous (in one cycle) effects of changing the mechanical conditions of contraction, as opposed to experiments with changes in preload in isometric twitches, where the effects associated with the accumulation of cycle-by-cycle changes in the behavior of the cardiomyocyte were revealed.

Modelling the afterload shortening of a virtual cardiomyocyte in the new integrative model, as in the *TP+M* model [7], reproduces the effect of inactivation of muscle contractility in response to a decrease in the applied load experimentally observed on laboratory animal heart preparations [21]. Figures 5a and 5b demonstrate this effect. With a decrease in the applied afterload (Fig. 5b), the rate of muscle isotonic relaxation increases. As a result, the smaller the afterload, the greater the difference between the duration of the isotonic shortening–lengthening phase and the duration of the period of steady-state isometric twitch, during which the generated force is higher than

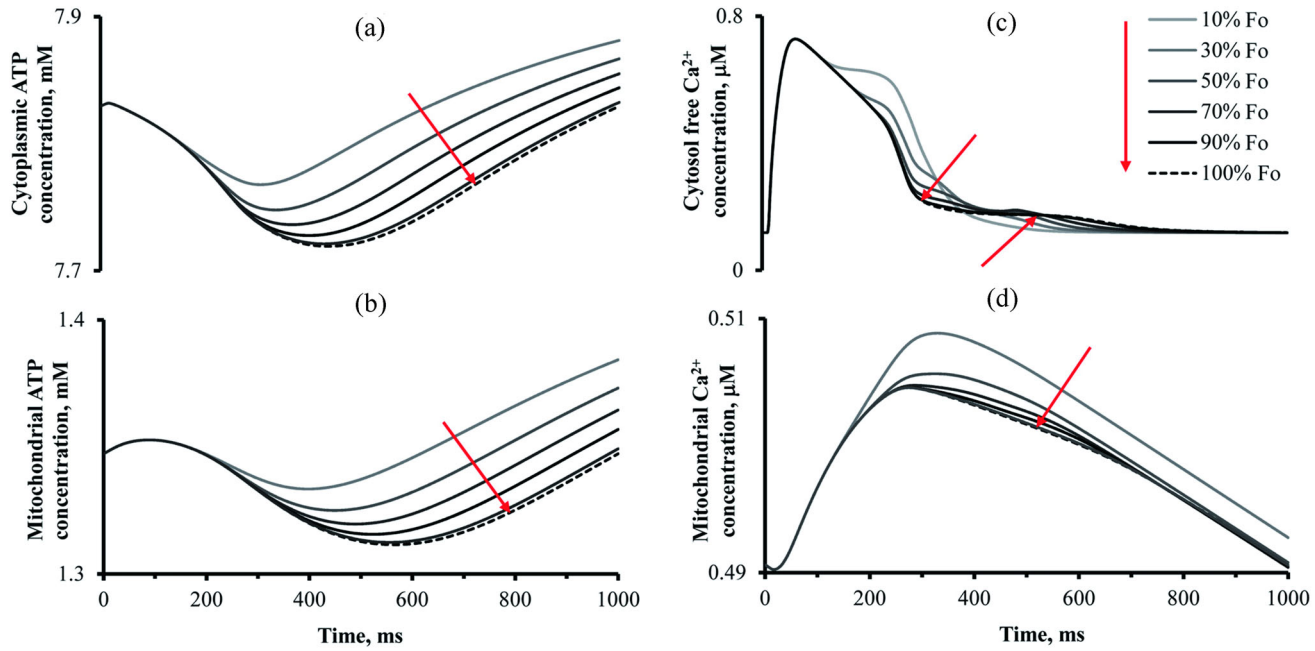

Fig. 6. Load dependence in the integrative model. The time course of changes in the ATP concentration in the cytosol (a) and in the mitochondria (d), and the concentration of calcium in the cytosol (c) and in the mitochondria (d) in steady-state isometric contraction (dotted lines) and at different afterloads (solid lines). The initial length of the virtual cardiomyocyte L_{init} = 90% L_{max}. F_0 is the maximum value of the isometric force developed by the cardiomyocyte at the initial length L_{init}. The afterload level is set in fractions of F_0. The arrows show the direction of displacement of the curves with increasing afterload.

the level of applied afterload (Fig. 5a).

We have previously shown that the mechanisms of ECC and MEF provide membrane potential change with a decrease in afterload during one cycle of isotonic contraction relative to the isometric twitch. The new integrative model reproduces this effect as well. Figure 5c shows that the AP duration in the new model has the highest value at the lowest used afterload. As the load increases, the AP duration begins to decrease, reaching the values of the isometric AP, which is 20 ms (7%) less than with the smallest afterload $\rho = 0.1F_0$.

The new integrative model shows that the characteristics of the metabolic module are also load-dependent. The mitochondrial membrane potential (Fig. 5d) at low afterloads during the period corresponding to the AP repolarization phase is less than its isometric values. Then, when AP passes into the resting potential, the mitochondrial membrane potential becomes higher than its isometric values. These changes may result from responding to load-dependent alterations in the time course of intracellular calcium concentration (Fig. 6c), affecting calcium transporters across the mitochondrial membrane.

Briefly, the crossover of the curves of the time course of changes in cytosolic calcium (Fig. 6c) during isotonic contractions is related to the mechano-dependence of the kinetics of CaTnC complexes. At the time of the crossover, very few CaTnC complexes remain bound, and therefore their decay almost stops for contractions under small afterloads as opposed to large afterloads. Therefore, after crossover, the smaller the load, the smaller intake of free calcium from the decaying CaTnC complexes into the cytosol. Such crossover of calcium signals at different afterloads was observed in experiments on rat cardiomyocytes [22]. The rate of calcium decline to diastolic levels is the result of a balance between mechanisms of calcium excretion from the cytosol (see equation (2)). The time course of the change in calcium flux through the mitochondrial sodium-calcium exchanger also exhibits a crossover (not shown) because the rate of its operation V_{NaCa}^{mit} is inversely proportional to the cytosolic calcium concentration: the higher the cytosolic calcium level, the lower its rate. Since, according to equa-

tion (13), the V_{NaCa}^{mit} is electrogenic, its changes result in the appearance of a crossover of the curves of the time course of changes in mitochondrial potential for different afterloads (Fig. 5d).

The acceleration of the CaTnC complexes decomposition under low loads, caused by the acceleration of isotonic relaxation, results in the additional free cytosol calcium, which enters the mitochondria through a calcium uniporter, also increasing the level of calcium in it (Fig. 6d).

Figures 6a and 6b present the time course of the ATP concentration changes in the cytosol and the mitochondria. As can be seen from the figure, the lower the afterload, the less the mentioned ATP concentrations change in the cycle. In our model, this can be explained by the direct proportionality of the rate of ATP hydrolysis by actomyosin ATPase V_{AM} to the number of cross-bridges formed (equation (7)). Therefore, the lower the force is held in afterload contractions, the lower the concentration of cross-bridges, and the lower the consumption of ATP by actomyosin ATPase. The exchange of ADP/ATP with mitochondria (equation (8)) makes it possible to maintain a higher level of ATP in the mitochondria (Fig. 6b) at low afterloads.

DISCUSSION

An integrative mathematical model has been constructed. The model describes in detail the electrical, mechano-chemical and metabolic processes in the human ventricular cardiomyocyte. Previously, some research groups developed integrative mathematical models that contain differently detailed descriptions of mechanisms of ECC, mitochondrial function and metabolic processes in cardiomyocytes [4, 2–25].

In these models, the influence of the frequency of stimulation as one of the fundamental factors determining the effective functioning of the heart was most often studied. A model of Hatano et al. [23] was used for study frequency-dependence of the electrical, energetic, and mechanical dynamics of individual cells of a 3D sample. In addition, they demonstrated the spatial distribution of calcium, force, and ADP_i during unloaded shortening and in isometric mode. However, the effect of mechanical conditions (isometry and unloaded contraction) was evaluated only by using the time course of changes in the calcium concentration in different compartments of the 3D sample. In addition, the model of Matsuoka et al. reproduces the effect of anoxia on metabolite concentrations and sarcomere shortening [25].

We selected one of the models of the Cortassa et al. group [4] as a basis for the construction of our integrative model [4]. The *Cortassa-2006* model [4] is based on their own metabolic model [26] and the ECC model of the guinea pig of Rice et al. [10, 11]. This *Cortassa-2006* model is more detailed, well-validated, and contains a description of the consumption of ATP in the cytosol. This consumption is taken into account in the overall balance of ATP/ADP in the cytosol and mitochondria. Such a detailed description allowed us to analyze the effect of ECC and MEF on the energy consumption of a cardiomyocyte. It will also allow us to further use a new integrative model for modelling cardiac pathologies associated with impaired oxygen consumption (hypoxia, ischemia, etc.).

When constructing our integrative model, the module used in the *Cortassa-2006* model to describe the electromechanical coupling in a guinea pig cardiomyocyte [10, 11] was replaced with the corresponding module from the *TP+M* model of a human cardiomyocyte. We have changed some parameters of the integrative model for the correct simulation of experimental data.

Using the developed integrative model, we demonstrated that a change in the mechanical conditions of contraction of a virtual cardiomyocyte affects not only its force generation and AP but also metabolic processes. Such changes are observed in response to an instantaneous change in the mechanical conditions of contraction (for example, in isotonic afterload contractions, Figs. 5, 6) and in the steady-state conditions (for example, in isometric twitches at different initial lengths, Figs. 1–4). It has been shown that in a healthy myocardium, the ATP level in the simulated myocytes is both length-dependent and load-dependent. In particular, the load-dependent changes in ATP are comparable to ATP variations during the isotonic twitches themselves. Meanwhile, the observed mechano-dependent

changes remain within 7.7–7.9 mM for cytosolic ATP and 1.35–1.45 mM for mitochondrial ATP, except in the case of the biggest preload corresponding to 95% of $L_{\max}$ (see Fig. 4) where cytosolic ATP was around 6.8 mM and the mitochondrial one 1.1 mM. This modest mechano-dependence may support the hypothesis that under normal physiological conditions the mechano-calcium, mechano-electro, and mechano-energy feedbacks in the cardiomyocyte are balanced such that ATP in the cytosol is maintained at a reliable level sufficient for all mechanical conditions of contraction [27]. The question of whether this balance, which provides an energy resource for the contraction, is preserved in ischemia will be investigated in the model later. We also plan to study the effect of the stimulation frequency on the metabolic and electromechanical activity of a healthy and pathological human ventricular cardiomyocyte in the model.

Figure 7 shows mechanisms and mediators involved in the cardiomyocyte in the realization of direct and feedback links between mechanical, electrical and metabolic processes in the integrative model of the human ventricular cardiomyocyte. The diagram was built entirely on the basis of the equations of the combined modules: *TP+M* model and *Cortassa-2006* model, taking into account the dependencies between the intracellular processes considered therein. The diagram also takes into account the direct and feedback relationships resulting from the combination of the models, described in the section "INTEGRATIVE MATHEMATICAL MODEL". For details on the construction of both combined models and the corresponding dependencies, we refer to the relevant publications describing development of the electrophysiological model *ten Tusscher-Panfilov-2006* [8, 28], the mechanical model *TP+M* [9, 12], and the metabolic model *Cortassa-2006* [4, 26]. The complete set of equations of the integrative model is included in the Supplementary Material.

The integrative models describe the main processes determining the function of the cardiac cell. They are as follows: Force generation by the cardiomyocyte and Sarcomere shortening; electrical potential across the cell membrane, changing in response to excitation signal (Membrane Potential); electrical potential across the mitochondrial membrane, determining its functional state (Mitochondrial membrane potential).

The main intermediaries involved in the realization of direct and feedback links are as follows: concentrations of ATP and ADP in the cytosol and mitochondria (ATP_i, ADP_i, ATP_m, ADP_m); concentrations of cytosolic and mitochondrial calcium (Ca_i and Ca_m); concentration of calcium-troponin complexes (CaTnC); concentration of force-generating cross-bridges (N_{XB}); coenzyme NADH involved in redox reactions, affecting the formation of enzyme in the tricarboxylic acid cycle (TCA cycle intermediates).

The main mechanisms through which the mutual influence of processes is carried out are as follows: calcium-dependent calcium currents (Ca_i-dependent Ca^{2+} currents), including the ATP-dependent current through a membrane calcium pump (i_{pCa}); ATP-dependent current through a sodium-potassium membrane pump (i_{NaK}); current through a ATP-sensitive potassium channel (i_{KATP}); ATP-dependent flow through the SR calcium pump (J_{up}); rate of ATP hydrolysis by myofibrils (V_{AM}); rates of calcium transfer across the mitochondrial membrane by a sodium-calcium antiporter and a calcium uniporter (V_{NaCa} and V_{uni}); rate of the adenine nucleotide translocator (V_{ANT}); rate of mitochondrial ATP synthase (V_{ATPase}); rate of proton transfer across ATP synthase (V_{Hu}); rate of respiratory chain proton pumping (V_{HNE}); rate of oxygen consumption (V_{O2}); rate of conversion of succinyl-CoA to succinate during hydrolysis (V_{SL}); rates of reactions in the tricarboxylic acid cycle associated with isocitrate dehydrogenase and α-ketoglutarate (V_{IDH} and V_{KGDH}).

Earlier, we carried out an analysis of the mutual influence of electrical and mechanical phenomena in cardiomyocytes [12, 29, 30]. Intracellular calcium plays a significant role in these interactions (Fig. 7, left part of the diagram). Its concentration during the contraction-relaxation cycle determines the amount of calcium–troponin complexes formed. The number of force-generating cross-bridges (N_{XB}) is determined by the available binding sites on actin resulting from the formation of CaTnC complexes, the sliding velocity of thin sarcomere filaments along the

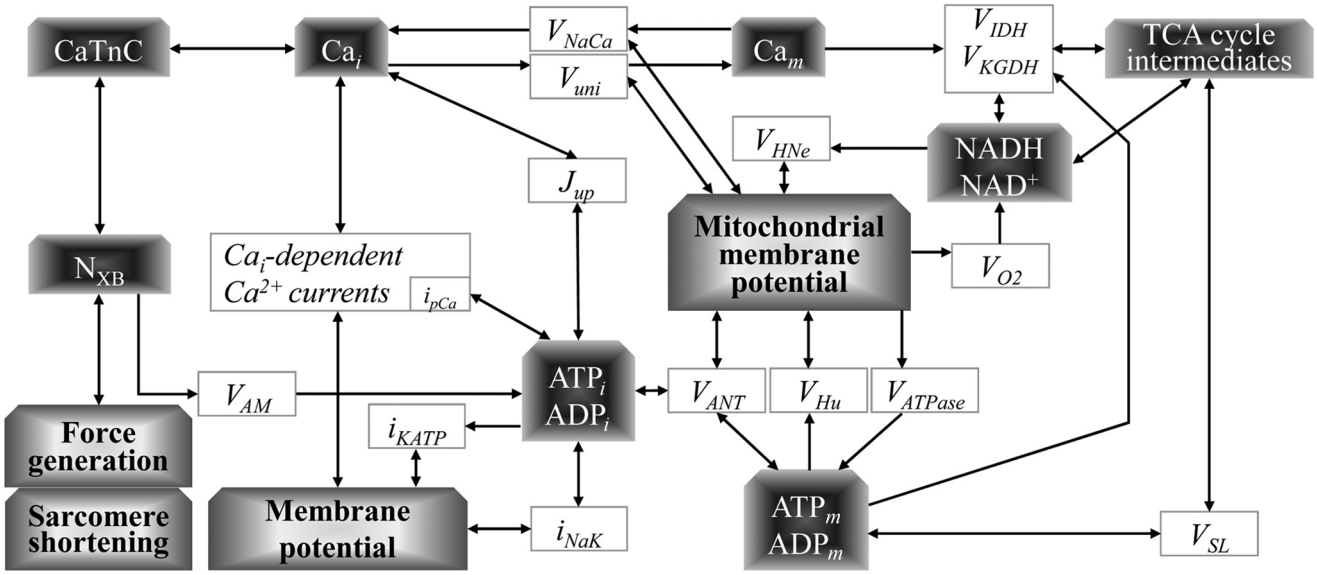

Fig. 7. Interrelation of processes in the electro-mechano-metabolic integrative model of the human ventricular cardiomyocyte. Three different groups of frames are for (1) the main processes that determine the function of the cell (shaded frames with black text); (2) the main intermediaries in the system of direct and feedback processes in the model (shaded frames with white text); and (3) the main mechanisms through which the mutual influence of processes is carried out (unshaded frames). The direction of the arrows corresponds to the direction of influence on the processes, mechanisms, and quantitative and temporal characteristics of the elements in the scheme. See the text for further details.

thick ones and the degree of their overlap. On the other hand, the lower the concentration of cross-bridges attached to thin filaments near the CaTnC complex, the faster decay of this complex (cooperativity mechanism accounted for in the model). These mechanisms provide mechano-calcium forward and reverse effects.

In addition to force generation, calcium plays a significant role in the generation of the cell membrane AP. Changes in the intracellular calcium concentration (Fig. 7, Ca_i) alter calcium-dependent membrane currents, determining the duration and amplitude of the AP, which affects all potential-dependent currents, including calcium-dependent ones.

Direct and inverse relations between electromechanical and metabolic processes are implemented in the model by (a) buffering cytosolic calcium by mitochondria; (b) ATP utilization in energy-dependent ECC processes.

When the mechanical conditions of cardiomyocyte contractions change, cooperative mechanisms of mechano-calcium feedback alter the amplitude and duration of the calcium transient. The calcium exchange between the cytosol and mitochondria affects the level of mitochondrial calcium (Fig. 7, Ca_m). Mitochondrial calcium regulates the rate of NADH production in the tricarboxylic acid cycle.

The model includes ATP-consuming processes, which play a role at different stages of ECC and MEF. The amount of ATP in the cytosol depends on the activity of these processes (Fig. 7, ATP_i). In particular, the calcium translocation by the SR pump (Fig. 7, J_{up}) and the membrane pump (Fig. 7, i_{pCa}), being dependent on cytosolic calcium, requires energy for the pumps to operate. The i_{pCa} current affects the membrane potential as well. The velocity of the sodium-calcium pump (Fig. 7, i_{NaK}) also depends on ATP and affects the membrane potential. The ATP-sensitive potassium current (Fig. 7, i_{KATP}) is inactive in healthy cardiac tissue. However, it can significantly increase during anoxia when ATP become less available. This increase in i_{KATP} can significantly affect AP duration and resting membrane potential in ischemic conditions.

The model does not describe the ATP-dependence of the detachment of the force-generating cross-bridges. However, the model accounts for

the consumption of ATP by the actomyosin ATPase (Fig. 7, V_{AM}). The transport of ATP through the mitochondrial membrane (Fig. 7, V_{ANT}) is another link between electromechanical and metabolic processes. In addition, V_{ANT} maintains the required level of ATP in the cytosol due to the ATP translocation from mitochondria to the cytosol and the ADP return to the mitochondria. The ATP/ADP transfer process affects the mitochondrial membrane potential. The obtained difference of electrochemical potentials on the mitochondrial membrane serves as a mover for the operation of ATP synthase (Fig. 7, V_{ATPase}) and the transfer of hydrogen protons (Fig. 7, V_{Hu}, V_{HNe}), as well as the processes of calcium transfer through the mitochondrial membrane (Fig. 7, V_{NaCa}, V_{uni}). One of the main processes of mitochondrial metabolism is cellular respiration. It also depends on the mitochondrial potential and governs the NADH level, which ultimately determines the rates of enzymatic reactions in the tricarboxylic acid cycle. In addition, some of these reactions are affected by the ADP/ATP level in mitochondria.

Thus, the developed model describes a large number of mechanisms that provide electromechanical-metabolic interaction in human ventricular cardiomyocytes. It can be used to explain physiological and pathophysiological phenomena in the heart on the cellular level and to hypothesize about underlying mechanisms. However, it is worth noting that the model has its limitations.

In particular, the model does not describe the function of mechanosensitive ion channels. These membrane channels activate in response to changes in mechanical conditions of contraction. Mechanosensitive current can contribute to slow, cycle-to-cycle AP changes in response to cardiomyocyte deformation [31]. Experimental evidence of the function of stretch-activated channels in cardiomyocytes remains contradictory (for more details, see [12]). We have argued (*ibidem*) that the length-dependent CaTnC complexes kinetics accounted for in our model rather than stretch-activated channels are responsible for the mechanical dependence of AP on preload under isometric conditions and afterload under isotonic conditions.

Another factor that could expand the model's applicability would be accounting for the role of nitric oxide (NO). NO is involved in many mechano-transduction pathways in the cardiomyocyte. NO regulates ion channel activity, calcium handling, cell energetics, etc [32]. Even though the NO synthesis from L-arginine does not require ATP energy, the reaction is oxygen-dependent. Therefore, when studying pathologies associated with insufficient blood supply to the myocardial tissue, taking into account the function of NO would be valuable.

Despite the limitations outlined above, the model is operational for studying the effects of pathological conditions, particularly those associated with ischemia (as the most common pathology of the cardiovascular system). In recent decades, numerous computational models have been developed describing the mechanisms of ischemia and reperfusion of the myocardium at different levels (from the cellular level to the level of the whole heart) [33–36]. Most of the models developed describe the effects of acute ischemia on myocardial electrophysiology, whereas the effects on myocardial contractile activity are poorly studied in the models. In the integrative model of the cardiomyocyte developed by Michailova and coauthors [37], the effect of metabolites in normal and pathological concentrations is studied not only on the time course and amplitude of ionic currents (i_{KATP}, i_{CaL}) and AP, but also on the kinetics of CaTnC complexes, which play an important regulatory role in force generation by cardiac muscle. Previously, we also used the guinea pig cardiomyocyte electromechanical model to study the electrical and mechanical activity of cardiomyocytes from different regions of the heart wall during the development of acute ischemia [38].

In the integrative model of electro-mechano-metabolic activity of a human cardiomyocyte that we have developed, it will be possible to simulate the factors observed under conditions of acute ischemia. In particular, we can simulate the effects of an increase in external potassium concentration [39] and acidosis associated with a decrease in the fast sodium current i_{Na} [40] and a decrease in the L-type calcium current i_{CaL} [41]. In addition, when the models were combined, a

description of the ATP-dependent current i_{KATP} was added, which is activated when ATP_i decreases due to hypoxia and acidosis [42].

Modeling of these factors may be used to study the processes of electromechanical coupling and bioenergetics during acute ischemia in human cardiomyocytes. The data obtained in such a study will help determine the role of mechano-dependence of intracellular processes in cardiomyocytes during ischemia and answer the questions of whether it is enhanced or attenuated, whether it plays a protective role in maintaining cell function, or whether it causes additional disorders.

CONCLUSIONS

We have developed an integrative model of the human ventricular cardiomyocyte that describes the complex relationships between the processes of its excitation, force generation, and metabolic processes within it. Within the framework of the model, it is shown that loading conditions affecting the contractile activity of the myocyte can both alter the course of electrophysiological processes in it and affect the processes of ATP production and consumption. The model can be used to simulate and analyze the subtle interrelationships of the processes observed in normal and pathological myocardium both at the level of a single cell and at the level of the whole heart when the cellular model is incorporated in three-dimensional models.

AUTHORS' CONTRIBUTION

Conceptualization and study design, data analysis, manuscript preparation—N.A.B.-V. and L.B.K.; models integration, writing software, performing numerical experiments, processing the results obtained—N.A.B.-V.

FUNDING

The study was supported by the Russian Science Foundation grant no. 21-14-00226.

CONFLICT OF INTEREST

The authors declare that they have no conflicts of interest.

SUPPLEMENTARY INFORMATION

The online version contains supplementary material available at https://doi.org/10.1134/S0022093022070122.

REFERENCES

1. Orini M, Nanda A, Yates M, Di Salvo C, Roberts N, Lambiase PD, Taggart P (2017) Mechano-electrical feedback in the clinical setting: Current perspectives. Prog Biophys Mol Biol 130: 365–375. https://doi.org/https://doi.org/10.1016/j.pbiomolbio.2017.06.001
2. Markhasin VS, Solov'eva O, Chumarnaia TV, Sukhareva SV (2009) The problem of myocardial heterogeneity. Ross Fiziol Zh Im I M Sechenova 95: 919–943.
3. Solovyova O, Katsnelson LB, Kohl P, Panfilov AV, Tsaturyan AK, Tsyvian PB (2016) Mechano-electric heterogeneity of the myocardium as a paradigm of its function. Prog Biophys Mol Biol 120: 249–254. https://doi.org/10.1016/j.pbiomolbio.2015.12.007
4. Cortassa S, Aon MA, O'Rourke B, Jacques R, Tseng H-J, Marbán E, Winslow RL (2006) A computational model integrating electrophysiology, contraction, and mitochondrial bioenergetics in the ventricular myocyte. Biophys J 91: 1564–1589. https://doi.org/10.1529/biophysj.105.076174
5. Brandes R, Bers DM (1999) Analysis of the mechanisms of mitochondrial NADH regulation in cardiac trabeculae. Biophys J 77: 1666–1682. https://doi.org/10.1016/S0006-3495(99)77014-1
6. Tinker A, Aziz Q, Thomas A (2014) The role of ATP-sensitive potassium channels in cellular function and protection in the cardiovascular system. Br J Pharmacol 171: 12–23. https://doi.org/10.1111/bph.12407
7. Bazhutina A, Balakina-Vikulova NA, Kursanov A, Solovyova O, Panfilov A, Katsnelson LB (2021) Mathematical modelling of the mechano-electric coupling in the human cardiomyocyte electrically connected with fibroblasts. Prog Biophys Mol Biol 159: 46–57. https://doi.org/10.1016/j.pbiomolbio.2020.08.003
8. ten Tusscher KH, Panfilov AV (2006) Alternans and spiral breakup in a human ventricular tissue model. Am J Physiol Heart Circ Physiol 291: H1088–H1100. https://doi.org/10.1152/ajpheart.00109.2006
9. Sulman T, Katsnelson LB, Solovyova O, Markha-

sin VS (2008) Mathematical modeling of mechanically modulated rhythm disturbances in homogeneous and heterogeneous myocardium with attenuated activity of Na^+–K^+ pump. Bull Math Biol 70: 910–49. https://doi.org/10.1007/s11538-007-9285-y

10. Jafri MS, Rice JJ, Winslow RL (1998) Cardiac Ca^{2+} dynamics: the roles of ryanodine receptor adaptation and sarcoplasmic reticulum load. Biophys J 74(3): 1149–1168. https://doi.org/10.1016/S0006-3495(98)77832-4
11. Rice JJ, Jafri MS, Winslow RL (2000) Modeling short-term interval-force relations in cardiac muscle. Am J Physiol Heart Circ Physiol 278: H913–H931. https://doi.org/10.1152/ajpheart.2000.278.3.H913
12. Balakina-Vikulova NA, Panfilov A, Solovyova O, Katsnelson LB (2020) Mechano-calcium and mechano-electric feedbacks in the human cardiomyocyte analyzed in a mathematical model. J Physiol Sci 70: 12. https://doi.org/10.1186/s12576-020-00741-6
13. Regnier M, Martyn DA, Chase PB (1998) Calcium regulation of tension redevelopment kinetics with 2-deoxy-ATP or low [ATP] in rabbit skeletal muscle. Biophys J 74: 2005–2015. https://doi.org/10.1016/S0006-3495(98)77907-X
14. Rice JJ, Winslow RL, Hunter WC (1999) Comparison of putative cooperative mechanisms in cardiac muscle: length dependence and dynamic responses. Am J Physiol 276: H1734–1754. https://doi.org/10.1152/ajpheart.1999.276.5.H1734
15. Vahl C, Timek T, Bonz A, Fuchs H, Dillman R, Hagl S (1998) Length dependence of calcium-and force-transients in normal and failing human myocardium. J Mol Cell Cardiol 30: 957–966. https://doi.org/10.1006/jmcc.1998.0670
16. Pieske B, Sutterlin M, Schmidt-Schweda S, Minami K, Meyer M, Olschewski M, Holubarsch C, Just H, Hasenfuss G (1996) Diminished post-rest potentiation of contractile force in human dilated cardiomyopathy. Functional evidence for alterations in intracellular Ca^{2+} handling. J Clin Invest 98: 764–776. https://doi.org/10.1172/JCI118849
17. Brixius K, Hoischen S, Reuter H, Lasek K, Schwinger RH (2001) Force/shortening-frequency relationship in multicellular muscle strips and single cardiomyocytes of human failing and nonfailing hearts. J Card Fail 7: 335–341. https://doi.org/S1071916401657026 [pii]
18. Yabe T, Mitsunami K, Inubushi T, Kinoshita M (1995) Quantitative Measurements of Cardiac Phosphorus Metabolites in Coronary Artery Disease by ^{31}P Magnetic Resonance Spectroscopy. Circulation 92: 15–23. https://doi.org/doi:10.1161/01.CIR.92.1.15
19. Page G, Ratchada P, Miron Y, Steiner G, Ghetti A, Miller PE, Reynolds JA, Wang K, Greiter-Wilke A, Polonchuk L, Traebert M, Gintant GA, Abi-Gerges N (2016) Human ex-vivo action potential model for pro-arrhythmia risk assessment. J Pharmacol Toxicol Methods 81: 183–195. https://doi.org/10.1016/j.vascn.2016.05.016
20. Vahl CF, Timek T, Bonz A, Kochsiek N, Fuchs H, Schaffer L, Rosenberg M, Dillmann R, Hagl S (1997) Myocardial length-force relationship in end stage dilated cardiomyopathy and normal human myocardium: analysis of intact and skinned left ventricular trabeculae obtained during 11 heart transplantations. Basic Res Cardiol 92: 261–270. https://doi.org/10.1007/BF00788521
21. Izakov V, Katsnelson LB, Blyakhman FA, Markhasin VS, Shklyar TF (1991) Cooperative effects due to calcium binding by troponin and their consequences for contraction and relaxation of cardiac muscle under various conditions of mechanical loading. Circ Res 69: 1171–1184. https://doi.org/10.1161/01.RES.69.5.1171
22. Yasuda S, Sugiura S, Yamashita H, Nishimura S, Saeki Y, Momomura S, Katoh K, Nagai R, Sugi H (2003) Unloaded shortening increases peak of Ca^{2+} transients but accelerates their decay in rat single cardiac myocytes. Am J Physiol Heart Circ Physiol 285: H470–475. https://doi.org/10.1152/ajpheart.00012.2003
23. Hatano A, Okada J, Washio T, Hisada T, Sugiura S (2011) A three-dimensional simulation model of cardiomyocyte integrating excitation-contraction coupling and metabolism. Biophys J 101: 2601–2610. https://doi.org/10.1016/j.bpj.2011.10.020
24. Youm JB, Choi SW, Jang CH, Kim HK, Leem CH, Kim N, Han J (2011) A computational model of cytosolic and mitochondrial [Ca^{2+}] in paced rat ventricular myocytes. Korean J Physiol Pharmacol 15: 217–239. https://doi.org/10.4196/kjpp.2011.15.4.217
25. Matsuoka S, Sarai N, Jo H, Noma A (2004) Simulation of ATP metabolism in cardiac excitation–contraction coupling. Prog Biophys Mol Biol 85: 279–299. https://doi.org/10.1016/j.pbiomolbio.2004.01.006
26. Cortassa S, Aon MA, Marban E, Winslow RL, O'Rourke B (2003) An integrated model of cardiac mitochondrial energy metabolism and calcium dynamics. Biophys J 84: 2734–2755. https://doi.org/10.1016/S0006-3495(03)75079-6
27. Saks V, Dzeja P, Schlattner U, Vendelin M, Ter-

zic A, Wallimann T (2006) Cardiac system bioenergetics: metabolic basis of the Frank-Starling law. J Physiol 571: 253–273. https://doi.org/10.1113/jphysiol.2005.101444
28. ten Tusscher KH, Noble D, Noble PJ, Panfilov AV (2004) A model for human ventricular tissue. Am J Physiol Heart Circ Physiol 286: H1573–1589. https://doi.org/10.1152/ajpheart.00794.2003
29. Solovyova O, Vikulova N, Katsnelson LB, Markhasin VS, Noble P, Garny A, Kohl P, Noble D (2003) Mechanical interaction of heterogeneous cardiac muscle segments in silico: effects on Ca^{2+} handling and action potential. Int J Bifurcat Chaos 13: 3757–3782. https://doi.org/10.1142/S0218127403008983
30. Solovyova O, Vikulova N, Markhasin V, Kohl P (2003) A novel method for quantifying the contribution of different intracellular mechanisms to mechanically induced changes in action potential characteristics. LNCS 2674: 8–17. https://doi.org/10.1007/3-540-44883-7_2
31. Peyronnet R, Nerbonne JM, Kohl P (2016) Cardiac Mechano-Gated Ion Channels and Arrhythmias. Circ Res 118: 311–329. https://doi.org/10.1161/CIRCRESAHA.115.305043
32. Boycott HE, Nguyen MN, Vrellaku B, Gehmlich K, Robinson P (2020) Nitric Oxide and Mechano-Electrical Transduction in Cardiomyocytes. Front Physiol 11: 606740. https://doi.org/10.3389/fphys.2020.606740
33. Ch'en FF, Vaughan-Jones RD, Clarke K, Noble D (1998) Modelling myocardial ischaemia and reperfusion. Prog Biophys Mol Biol 69: 515–538. https://doi.org/10.1016/S0079-6107(98)00023-6
34. Crampin EJ, Smith NP, Langham AE, Clayton RH, Orchard CH (2006) Acidosis in models of cardiac ventricular myocytes. Philos Trans R Soc Lond A 364: 1171–1186. https://doi.org/doi:10.1098/rsta.2006.1763
35. Rodriguez B, Ferrero JM Jr, Trenor B (2002) Mechanistic investigation of extracellular K^+ accumulation during acute myocardial ischemia: a simulation study. Am J Physiol Heart Circ Physiol 283: H490–H500. https://doi.org/10.1152/ajpheart.00625.2001
36. Loewe A, Wülfers EM, Seemann G (2018) Cardiac ischemia—insights from computational models. Herzschrittmacherther Elektrophysiol 29: 48–56. https://doi.org/10.1007/s00399-017-0539-6
37. Michailova A, Saucerman J, Belik ME, McCulloch AD (2005) Modeling regulation of cardiac KATP and L-type Ca^{2+} currents by ATP, ADP, and Mg^{2+}. Biophys J 88: 2234–2249. https://doi.org/10.1529/biophysj.104.046284
38. Vikulova NA, Vasilyeva AD, Zamaraev DE, Solovyova OE, Markhasin VS (2014) Modeling of disturbances in electrical and mechanical function of cardiomyocytes under acute ischemia. Biophysics 59: 791–799. https://doi.org/10.1134/s0006350914050297
39. Weiss JN, Venkatesh N, Lamp ST (1992) ATP-sensitive K^+ channels and cellular K^+ loss in hypoxic and ischaemic mammalian ventricle. The Journal of Physiology 447: 649–673. https://doi.org/10.1113/jphysiol.1992.sp019022
40. Kagiyama Y, Hill JL, Gettes LS (1982) Interaction of acidosis and increased extracellular potassium on action potential characteristics and conduction in guinea pig ventricular muscle. Circ Res 51: 614–623. https://doi.org/10.1161/01.RES.51.5.614
41. Irisawa H, Sato R (1986) Intra- and extracellular actions of proton on the calcium current of isolated guinea pig ventricular cells. Circ Res 59: 348–355. https://doi.org/10.1161/01.res.59.3.348
42. Noma A (1983) ATP-regulated K^+ channels in cardiac muscle. Nature 305: 147–148. https://doi.org/10.1038/305147a0

Translated by A. Polyanovsky